THE JOURNAL OF PHYSICAL CHEMISTRY A

A: Molecular Structure, Quantum Chemistry, and General Theory

Effect of Coulomb Correlation on the Magnetic Properties of Mn Clusters

Chengxi Huang, Jian Zhou, Kaiming Deng, Erjun Kan, and Puru Jena

J. Phys. Chem. A, **Just Accepted Manuscript** • Publication Date (Web): 18 Apr 2018

Effect of Coulomb Correlation on the Magnetic Properties of Mn Clusters

Chengxi Huang[1,2], Jian Zhou[2], Kaiming Deng[1], Erjun Kan[1,*], Puru Jena[2,*]

[1] *Department of Applied Physics and Key Laboratory of Soft Chemistry and Functional Materials (Ministry of Education), Nanjing University of Science and Technology, Nanjing, Jiangsu 210094, P. R. China*

[2] *Department of Physics, Virginia Commonwealth University, Richmond, Virginia 23284, United States*

Abstract

In spite of decades of research, a fundamental understanding of the unusual magnetic behavior of small Mn clusters remains a challenge. Experiments show that Mn_2 is *antiferromagnetic* while small clusters containing up to five Mn atoms are ferromagnetic with magnetic moments of 5 μ_B/atom, and become ferrimagnetic as they grow further. Theoretical studies based on density functional theory (DFT), on the other hand, find Mn_2 to be *ferromagnetic*, with ferrimagnetic order setting in at different sizes that depend upon the computational methods used. While quantum chemical techniques correctly account for the antiferromagnetic ground state of Mn_2, they are computationally too demanding to treat larger clusters, making it difficult to understand the evolution of magnetism. These studies clearly point to the importance of correlation and the need to find ways to treat it effectively for larger clusters and nanostructures. Here, we show that the DFT+*U* method can be used to account for strong correlation. We determine the on-site Coulomb correlation, Hubbard *U* self-consistently by using the linear response theory and study its effect on the magnetic coupling of Mn clusters containing up to 5 atoms. With a calculated *U* value of 4.8 eV, we show that the ground state of Mn_2 is *antiferromagnetic* with a Mn-Mn distance of 3.34 Å, which agrees well with the electron spin resonance experiment. Equally important, we show that on-site Coulomb

* E. K. (ekan@njust.edu.cn), P. J. (pjena@vcu.edu)

correlation also plays an important role in the evolution of magnetic coupling in larger clusters, as the results differ significantly from standard DFT calculations. We conclude that for a proper understanding of magnetism of Mn nanostructures (clusters, chains and layers) one must take into account the effect of strong correlation.

I. Introduction

Magnetic materials with large magnetic moments per atom are important for technological applications[1,2]. Since the magnetic moments are enhanced in reduced dimensions, there has been a long-standing interest to study the magnetic moments per atom in clusters, nanowires, and two-dimensional materials. Mn is an interesting element in this regard; owing to its atomic $3d^5\ 4s^2$ configuration, it binds weakly with other atoms and usually carries a magnetic moment of 5 μ_B/atom. Due to this reason, there is considerable interest in the design and synthesis of Mn-based ferromagnetic materials for use as magnetic storage and magnetic memory materials.

However, a fundamental understanding of the evolution of magnetism in Mn clusters has been challenging. For example, it has been difficult to predict even the ground state of Mn dimer (Mn_2). A previous experiment using the electron spin resonance (ESR) showed that Mn_2 prefers antiferromagnetic (AFM) coupling with a bond length of 3.2 Å.[3] However, calculations based on density functional theory (DFT) using generalized gradient approximation (BPW91) and hybrid functional (B3LYP) yield a ferromagnetic (FM) ground state with a much shorter bond length of ~2.6 Å.[4-11] The only theoretical result based on DFT that correctly predicts the ground magnetic state of the neutral Mn_2 dimer is due to Barborini[12] who used the BHHPW91 hybrid functional. The controversy becomes more complicated when the cluster becomes bigger, especially for Mn_5. While it is understood that Mn_4 is a ferromagnetic cluster[13] with a magnetic moment of 5 μ_B/atom, the magnetic moment of Mn_5 cluster is still an open question. In a previous ESR experiment, Mn_5 cluster, isolated in a matrix, was found to be FM with 5 μ_B/atom.[3,14] However, a more recent Stern-Gerlach molecular beam experiment claimed that Mn_5 prefers ferrimagnetic (FIM) coupling with a magnetic moment of 0.79±0.25 μ_B.[15] On the theoretical side, Nayak *et al*. predicted the Mn_5 cluster to be FM with a total magnetic moment of 25 μ_B.[4,5] Pederson *et al.* also obtained a FM ground state, but with a total spin moment of 23 μ_B.[6] On the contrary, recent DFT-based calculations by Kabir,

Gutsev, and their coworkers yield a FIM ground state with a total magnetic moment of 3 μ_B, i.e. 0.6 μ_B/atom.[9-11] In bulk α-Mn, each Mn atom only carries magnetic moment of 0.2 ~ 1.9 μ_B/atom, and the coupling between Mn atoms is antiferromagnetic.[16,17] Thus, to clearly understand the magnetic behavior of Mn clusters as well as Mn-based crystals, more accurate calculations are required.

It is well-known that 3*d* transition metals are strongly correlated systems due to the on-site repulsion effects of localized *d* orbitals. However, in most previous calculations[4-11] on Mn clusters, such strong electronic correlation was not properly treated. Recently quantum chemical calculation based on multi-reference method[18] did predict Mn_2 to be antiferromagnetic, but such methods are computer intensive and have not been applied to study larger clusters. One simple way to include strong correlation is to add an empirical Hubbard term (*U*) in the Kohn-Sham Hamiltonian (DFT+*U*), which has been well proved to improve the prediction compared with standard DFT calculations.[19-23] The value of *U* is usually estimated by comparing with the experiments. As the magnitude of *U* varies in different materials[24,25], and there are no experiments on clusters that can be used to estimate it, a way to obtain a reasonable *U* value, without experimental input, is to perform a self-consistent linear response calculation for a specific structure.[26] In the current study, we use such a method to determine the Hubbard *U* for the Mn_2 cluster, and adopt this value to study the magnetic properties of larger Mn clusters. With the *U* value of 4.8 eV, we obtain the same results as in the ESR experiment for Mn_2, i.e. AFM ground state with a Mn-Mn distance of 3.34 Å. This demonstrates that adding the Hubbard *U* is crucial to obtain the correct ground state of Mn_2. We then apply the same procedure to study larger Mn_x (x = 3-5) clusters. For comparison, we also calculate the magnetic properties by using the conventional DFT method. Very different results are obtained between DFT and DFT+*U* calculations. Furthermore, we analyze the effect of Hubbard *U* on the electronic structure by focusing on Mn_2 and Mn_5. Generally speaking, adding Hubbard *U* reduces the *s*-*d* hybridization, resulting in weaker binding and longer bond

length between Mn atoms. In addition, the increase of Mn-Mn bond length narrows the expansion of *d* orbitals in the energy space, thus, enlarging spin-splitting. We argue that the Hubbard *U* is mainly responsible for the magnetic state transitions, despite the geometry difference. A magnetic phase diagram as a function of average Mn-Mn bond length and Hubbard *U* for Mn_5 is presented to describe the unusual FIM-to-FM-to-FIM transition in Mn_5. We also present the magnetic properties of Mn_5^- and Mn_5^+ ions to discuss the environmental effect on the magnetic states of the cluster. Our calculations indicate that both Mn_5^- and Mn_5^+ are FIM with the total spin of 6 (1.2 μ_B/atom) and 4 μ_B (0.8 μ_B,), respectively. These results may explain the controversy associated with experimental results on the magnetic states of Mn_5.

II. Theoretical Methods

Our first-principles calculations are based on spin-polarized DFT with generalized gradient approximation (GGA) for the exchange-correlation functional.[27,28] We used linear response approach implemented in the Quantum-ESPRESSO (QE) code to determine the appropriate Hubbard *U* value self-consistently.[29] The cutoff energies for plane-wave function and charge density were set to be 80 and 960 Ry, respectively. Next, we used the Vienna *Ab initio* Simulation Package (VASP)[30] to calculate the geometric and electronic structures of Mn_x (x =2-5) clusters. The projector augmented wave (PAW) method[31] was used to treat the core electrons and the valence electrons were expanded using the plane-wave basis set with a cutoff energy of 400 eV. The effective Hubbard *U* was added using the Dudarev's method[32] for the Mn-*d* orbitals. Both Perdew-Burke-Ernzerhof (PBE)[27] and Perdew-Wang (PW91)[28] forms of GGA functionals were used and consistent results were obtained. The Vosko-Wilk-Nusair[33] interpolation scheme was included in order to obtain correct magnetic configuration. A vacuum space of 20 Å along all directions was adopted to model the isolated molecular system. The reciprocal space was represented by the Γ point. The convergence criteria for

energy and Hellmann-Feynman force component were set to be 1×10^{-5} eV and 0.01 eV/Å, respectively. Note that, our calculated energy differences are larger than 10 meV, which is within the accuracy of the DFT and DFT+*U* methods. For the charged clusters, dipole-dipole interaction corrections[34] were included.

III. Results and Discussions

We begin our analysis with the magnetism of Mn_2. Although it is the smallest and simplest Mn cluster, as stated in the introduction, the calculated ground state of Mn_2 is not consistent with the experimental results. Both the resonance Raman spectroscopy[35] and ESR[3] experiments showed that Mn_2 favors AFM coupling with a Mn-Mn distance of 3.17 Å, while almost all the previous DFT based calculations predicted a FM ground state with much shorter Mn-Mn distance (~2.6 Å). To verify previous theoretical results, we also performed spin-polarized DFT calculations using PBE and PW91 functionals and obtained the same FM ground state with Mn-Mn distance of 2.63 Å (using PBE) and 2.58 Å (using PW91). Inclusion of van der Waals (vdW) interaction corrections (DFT-D2)[36] did not change these results. Next, we introduced Hubbard *U* in the PW91 functional with the value of *U* ranging from 1 to 6 eV. As shown in Fig. 1, adding Hubbard *U* increases the Mn-Mn distance monotonically, and the exchange energy (defined as $E_{\text{FM-AFM}} = E_{\text{FM}} - E_{\text{AFM}}$) increases drastically. $U = 2$ eV represents a critical point where FM and AFM configurations are degenerate, and the Mn-Mn distance becomes 3.2 Å, indicating weak binding energy. When $U > 2$ eV, the exchange energy becomes positive, namely, the ground state converts to an AFM state. Further increasing *U* (up to 6 eV) retains the AFM ground state, and the Mn-Mn distance and exchange energy increase slightly (see the supporting information). Apparently, the calculated magnetic ground state of Mn_2 strongly depends on the value of Hubbard *U*. Very similar results were obtained when PBE+*U* method was adopted.

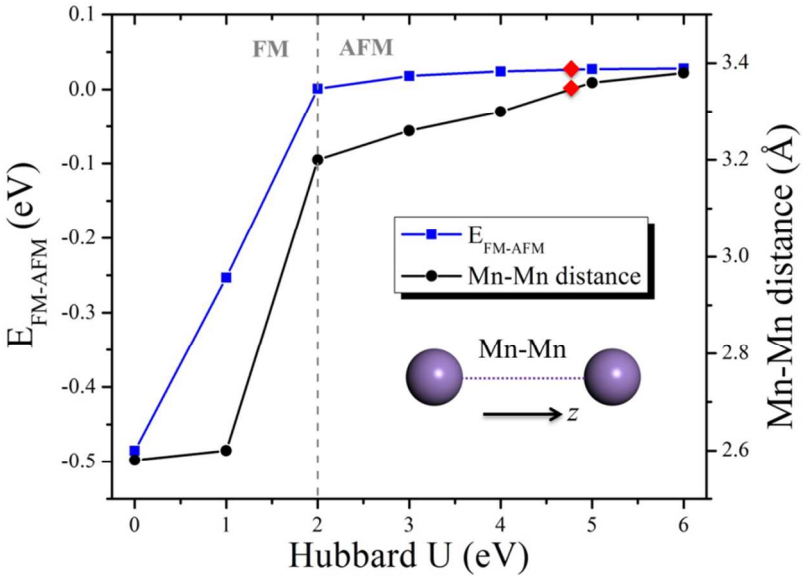

Figure 1. Energy difference between ferromagnetic (FM) and antiferromagnetic (AFM) states and Mn-Mn distance for Mn_2 as a function of Hubbard *U*. The red diamonds denote the results with *U* of 4.8 eV derived from linear response approach.

The value of *U* varies in different systems and different bonding environments. Therefore, in order to obtain the correct ground state, we use linear response method proposed by Cococcioni and Gironcoli to calculate the value of *U*.[26] The effective *U* is expressed as the difference of the second derivative of total energy with respect to occupation number in interacting and non-interacting Kohn-Sham equations,

$$U = \frac{d^2E\left[\left\{n^I\right\}\right]}{d\left(n^I\right)^2} - \frac{d^2E_0\left[\left\{n^I\right\}\right]}{d\left(n^I\right)^2}.$$

Here *E* and E_0 are total energy of the interacting and non-interacting Kohn-Sham equations, respectively, and n^I is the occupation number of localized *d*-orbital at site *I*. After calculation, we obtain an effective *U* value of 4.8 eV (see the supporting information for details). This corresponds to a weak AFM coupling with exchange energy of 26 meV. The calculated Mn-Mn distance of 3.3 Å is close to the experimental result of 3.2 Å.[3]

After studying the effect of Hubbard U on Mn_2, we now move to bigger Mn clusters. Table 1 lists the calculated results without and with Hubbard U for Mn_x (x = 2-5). When Hubbard U is not included, Mn_2 to Mn_4 clusters all show FM ground states which are much lower in energy than the AFM and FIM states. This agrees with previous DFT calculations.[4,8-10] Mn_5 exhibits an FIM ground state with a total magnetic moment of 3 μ_B. When Hubbard U = 4.8 eV is included, the ground state of Mn_2 and Mn_3 become AFM and FIM, but Mn_4 retains its FM ground state, although the energy differences between AFM and FM states are small (< 0.03 eV). Mn_5 becomes FM with a total magnetic moment of 25 μ_B. Besides the magnetic phases, distinct differences are also found in their vertical detachment energy (VDE) and vertical ionization potential (VIP) by using these two methods. These results further reveal that Hubbard U could drastically influence the magnetic and electronic states of small Mn clusters. Note that, spin-frustration and spin-orbit interaction may result in non-collinear spin order. However, for Mn clusters, this effect is usually very small compared to the magnetic exchange coupling.[37] Thus, here we focus on the spin collinear calculations.

Table 1. Effect of Hubbard U on the magnetism of Mn_x (x= 2~5) clusters. We list all the magnetic configurations considered in our calculations. Total magnetic moments (m_{tot} in μ_B), relative energy (ΔE, in eV), vertical detachment energy (VDE, in eV), and vertical ionization potential (VIP, in eV) are listed. For Mn_5 cluster, we list the magnetic configurations in parentheses.

	Without U				With U (4.8 eV)			
Structure	m_{tot}	ΔE	VDE	VIP	m_{tot}	ΔE	VDE	VIP
Mn_2	0	0.48	0.99	6.34	0	0.00	0.60	5.84
	10	0.00			10	0.03		
Mn_3	5	0.09	1.41	6.11	5	0.00	0.80	5.89
	15	0.00			15	0.01		
Mn_4	0	0.29	1.83	6.01	0	0.03	1.12	6.05
	10	0.15			10	0.02		
	20	0.00			20	0.00		

Mn_5	3 (M2)	0.00	1.59	5.61	5 (M2)	0.10	1.15	5.23
	5 (M4)	0.25			5 (M4)	0.20		
	5 (M5)	0.27			5 (M5)	0.28		
	13 (M3)	0.08			15 (M3)	0.08		
	13 (M6)	0.004			15 (M6)	0.10		
	23 (M1)	0.08			25 (M1)	0.00		

To understand how Hubbard U affects the magnetic properties of Mn clusters, we focus on Mn_5 whose ground state is still under intensive debate. In Fig. 2(a), we plot four possible magnetic configurations for the triangular bi-pyramid (TBP) geometry. The M1 state is FM, and the M2, M3, and M4 states are candidates for FIM states, according to previous calculations. Other possible geometries (square pyramid and pentagon) and magnetic configurations have much higher energies and can be found in the supporting information. The relative energies of these states using different functionals with and without vdW correction are listed in Table 2. Without Hubbard U, the FIM (M2) configuration with a total spin moment of 3 μ_B (0.6 μ_B/atom) has the lowest energy, and the FM (M1) state with 23 μ_B lies 0.08 eV higher [Fig. 2(b)]. The average Mn-Mn bond length (denoted as $d_{Mn\text{-}Mn}$ = 2.53 Å) is insensitive to the choice of GGA (PBE and PW91). The effect of vdW interaction on the geometric structure is also marginal. These facts are consistent with previous calculations. However, similar to the case of Mn_2, the inclusion of the strong correlation changes the relative energies of these magnetic states. After including Hubbard U of 4.8 eV, the FM (M1) state with 25 μ_B becomes the ground state of Mn_5, while the M2 state with 5 μ_B is 0.1 eV higher in energy [Fig. 2(c)]. From the optimized structures, we find that the $d_{Mn\text{-}Mn}$ is increased to ~3.02 Å after including Hubbard U (actually the structures also distort slightly after U is introduced). Such bond length increment is similar to the case of Mn_2 (from 2.58 to 3.34 Å). Again, these results do not change if PBE functional is adopted. In order to confirm our results, we repeated the calculations with U = 4.0 and 5.6 eV (Table 2). We find that the energy difference

between FM and M2 states decreases (increases) under larger (smaller) Hubbard *U*, but the ground state remains FM with a magnetic moment of 25 μ_B.

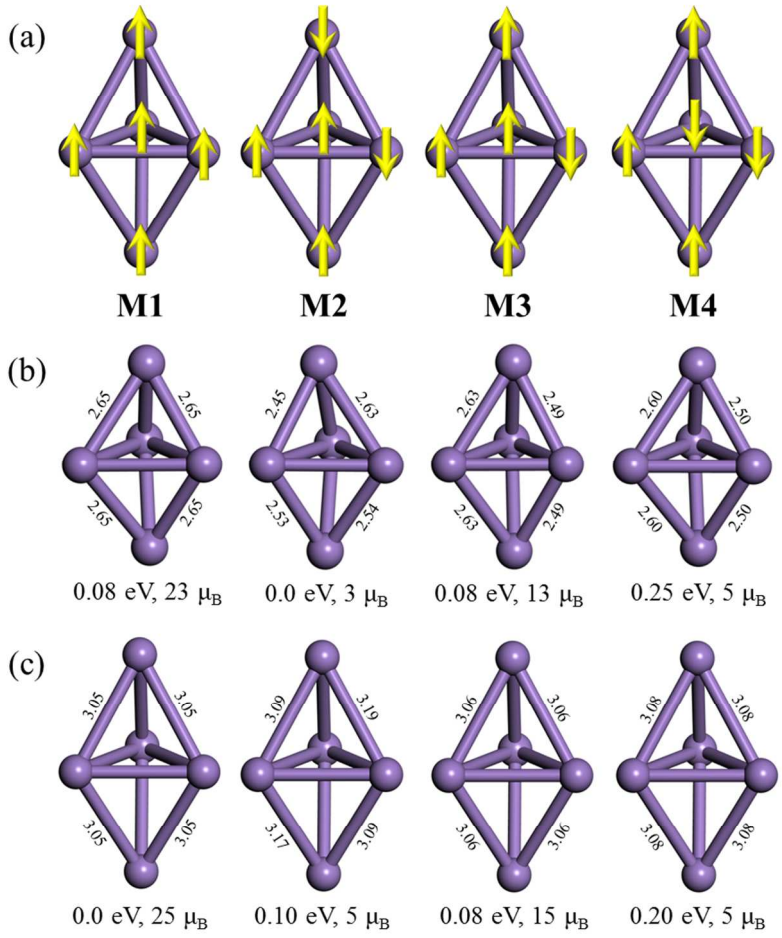

Figure 2. (a) Four different magnetic configurations for Mn_5. Optimized structures, relative energies and total magnetic moment for Mn_5 calculated using PW91+vdW method without (b) and with (c) Hubbard *U* of 4.8 eV. The bond lengths are represented in Å.

Table 2. Relative energies (E_{M1}, E_{M2}, E_{M3}, E_{M4}) of four magnetic configurations of Mn_5 and average Mn-Mn bond lengths ($d_{Mn\text{-}Mn}$) of the optimal configuration calculated using various functionals. The number in parenthesis is the value obtained including Hubbard U.

	E_{M1} (eV)	E_{M2} (eV)	E_{M3} (eV)	E_{M4} (eV)	$d_{Mn\text{-}Mn}$ (Å)
PBE	0.18	0	0.11	0.26	2.53
PW91	0.12	0	0.09	0.26	2.53
PW91+vdW	0.08	0	0.08	0.25	2.54
PW91+U (4.8)	0	0.13	0.08	0.18	2.94
PW91+vdW+U (4.8)	0	0.10	0.08	0.20	3.02
PBE+vdW+U (4.8)	0	0.10	0.08	0.19	3.02
PW91+vdW+U (4.0)	0	0.20	0.11	0.22	2.97
PW91+vdW+U (5.6)	0	0.02	0.05	0.12	3.07

We now discuss the effect of Hubbard U on the electronic structure of Mn_2 and Mn_5, and explore the physical origin of their magnetic states. Fig. 3 shows the partial density of states (PDOS) of a single Mn atom in Mn_2. We focus on the *s*-*d* hybridization and expansion of *d* orbitals in the energy space. In an isolated Mn atom, the five *d* orbitals are degenerate in energy, thus, the *d* orbitals are not expanded. When two Mn atoms are bonded, the *d* orbitals form bonding and antibonding states. Thus, the *d* orbitals of a Mn atom expand, which reflects the bonding between the Mn atoms. Without U [Fig. 3(a)], one sees a strong hybridization between *s* and *d* orbitals. Here only d_z^2 is plotted because the *s* and other *d* orbitals (d_{xy}, $d_{x^2-y^2}$, d_{xz}, and d_{yz}) have different eigenvalues under C_∞ operator and will not hybridize. When two Mn atoms form a dimer, the *s*-d_z^2 hybridization helps the formation of the bonding and antibonding state. Such hybridization yields small Mn-Mn distance (2.6 Å) with large binding energy (1.02 eV).

When the Hubbard U is introduced, the d orbitals are pushed far away from the Fermi level and the s orbital. Hence, the s-d_z^2 hybridization is greatly reduced [Fig. 3(b)], though bonding and antibonding molecular orbitals of Mn_2 are preserved (see the supporting information). Consequently, the Mn-Mn distance increases to 3.3 Å (in the range of vdW interaction), and the binding energy becomes very small (0.23 eV).

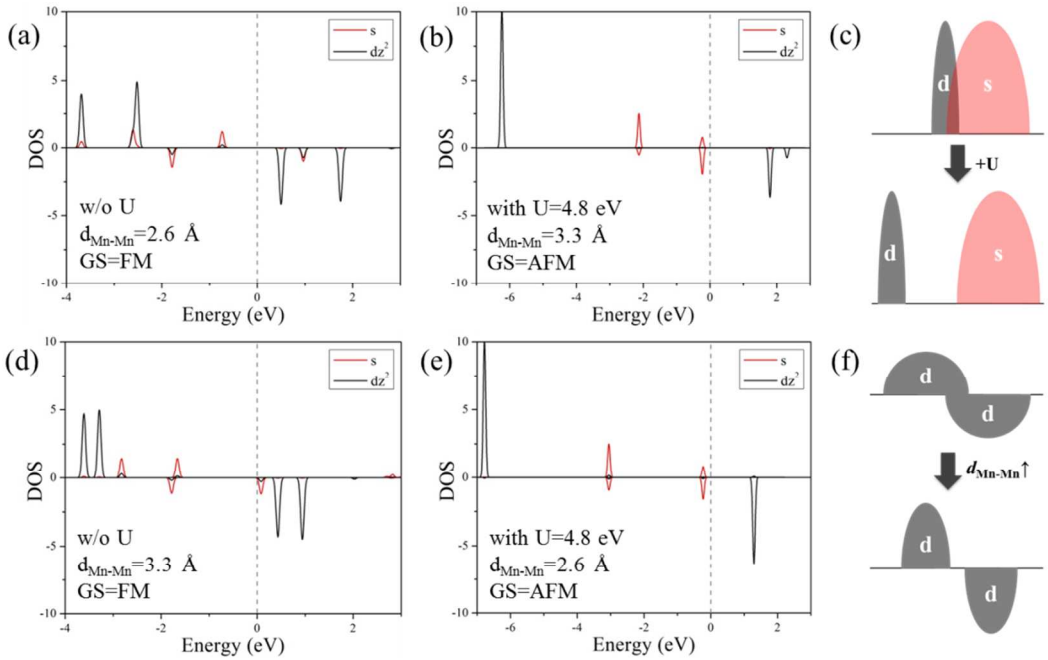

Figure 3. (a), (b), (d), (e) Partial density of states (PDOS) for single Mn atom of Mn_2. Schematic diagram of the effect of (c) Hubbard U and (f) Mn-Mn distance on the electronic structure of Mn_2.

The most dramatic effect after including Hubbard U is the changing of magnetic ground state of Mn_2 from FM to AFM. From the density of states, we have found that the energy level of s and d_z^2 orbitals and hybridizations between them depend on Hubbard U. Inclusion of Hubbard U enlarges the spin splitting and localizes the d orbitals, which diminishes their hybridization with other orbitals, e.g. the s-d_z^2 hybridization in our case. Keeping this in mind and to further reveal the mechanism of FM-to-AFM transition of the magnetic ground state for Mn_2 after including Hubbard U, we analyze the magnetic exchange interactions in this system based on the mean-field approximation (see Fig. 4).

When the Hubbard U is not included, the exchange splitting between $d_z^2\uparrow$ and $d_z^2\downarrow$ orbitals is relatively small. The d_z^2 orbitals can strongly hybridize with the s orbitals and the s orbital is spin-polarized. In this case, the exchange interactions between occupied $s\downarrow$ and empty $d_z^2\downarrow$ orbitals will stabilize the FM state. When Hubbard U is included, the exchange splitting of d orbitals is enlarged. The s-d_z^2 hybridization can be omitted so that the s orbitals are no longer spin-polarized. Thus, the exchange interactions only occur between d orbitals. Because the Mn-d orbitals are half-filled, the direct exchange interactions between them must be AFM (Fig. 4b).

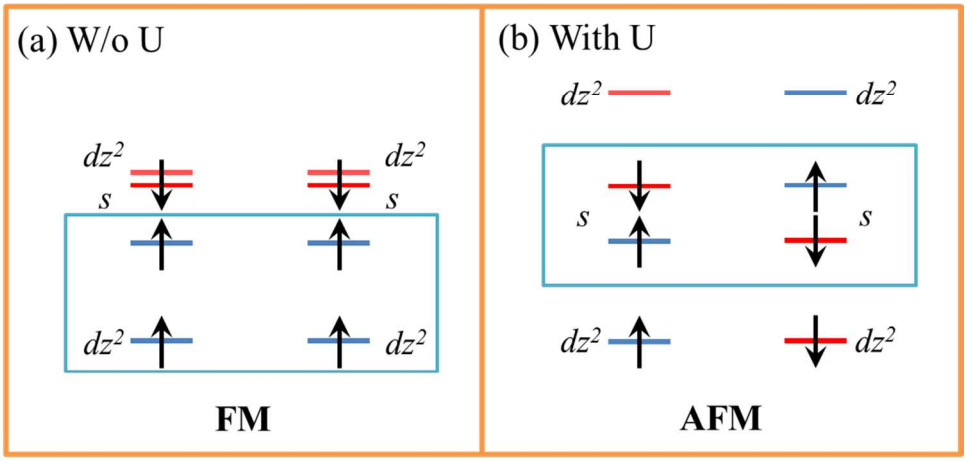

Figure 4. Schematic diagram of magnetic coupling in ferromagnetic (FM) and antiferromagnetic (AFM) alignments for the Mn_2 cluster based on the mean-field approximation. (a) When Hubbard U is not included. (b) When Hubbard U of 4.8 eV is included. Red and blue bars represent spin-down and spin-up orbitals. Black arrows represent the spins.

Previous studies have claimed that the exchange coupling between two Mn atoms in a semiconductor (e.g. GaN)[38] can be controlled by their distance. In the Mn_2 case, since $U = 0$ and $U = 4.8$ eV yield very different Mn-Mn distance, one may wonder if the calculated FM and AFM magnetic states are due to the geometry difference. To find out the answer, here we perform calculations with fixed Mn-Mn distance of 3.3 and 2.6 Å,

without and with Hubbard U. When Hubbard U is absent, the increase of Mn-Mn distance (from 2.6 to 3.3 Å) reduces the strength of s-d_z^2 hybridization [Fig. 3(d)] and the expansion of d orbitals in energy [Fig. 3(f)]. The exchange energy also increases from –0.48 eV to –0.13 eV, but the ground state remains FM. On the other hand, when the Hubbard U is included, the ground state of Mn_2 is always AFM, regardless of the Mn-Mn distance [Fig. 3(b) and (e)].

Next, we analyze the electronic structure of Mn_5, which is more complex because the five Mn atoms are not equivalent. Here, we only show PDOS of a single Mn atom of Mn_5, because the main features of PDOS for the five Mn atoms are similar. Fig. 5(a) shows the PDOS for FIM (M2) state without Hubbard U. One sees a large expansion of d orbitals in energy due to strong bonding between the Mn atoms having the TBP geometry. The spin up and spin down d states do not distinctly split in energy and the spin down d states are partially occupied. After including Hubbard U of 4.8 eV, the occupied and unoccupied states are separated in energy [Fig. 5(b)]. The expansion of d states in each spin channel is also reduced due to the increment of $d_{\text{Mn-Mn}}$ (from 2.53 to 3.02 Å). However, the s-d hybridization is still observed from the PDOS. If we continue to increase the value of Hubbard U to 7 eV, we observe no s-d hybridization (similar as in Mn_2 case of $U = 4.8$ eV) and the $d_{\text{Mn-Mn}}$ further increases (from 3.02 to 3.12 Å) [Fig. 5(c)]. The ground state changes to FIM (M2) again. Clearly, this FIM state (U = 7 eV) is different from the FIM state with $U = 0$ eV.

To explore the geometric effect, we calculated the magnetic coupling with the value of U fixed at 0 eV and 4.8 eV, while proportionally increasing the Mn-Mn bond length in Mn_5 (thus, increasing $d_{\text{Mn-Mn}}$) from their corresponding ground state value (i.e. FIM/M2 and FM/M1). We summarize these results in Fig. 5(d) where a clear FIM1-FM-FIM2 transition can be found. In the FIM1 state, the s-d hybridization is very strong and the expansion of d orbitals is large in energy, both corresponding to strong

Mn-Mn interaction. On the contrary, in the FIM2 state, the *s*-*d* hybridization is weak and the expansion of *d* orbitals is also small, giving longer Mn-Mn bond length. This is also same as the ground state of AFM Mn_2 cluster.

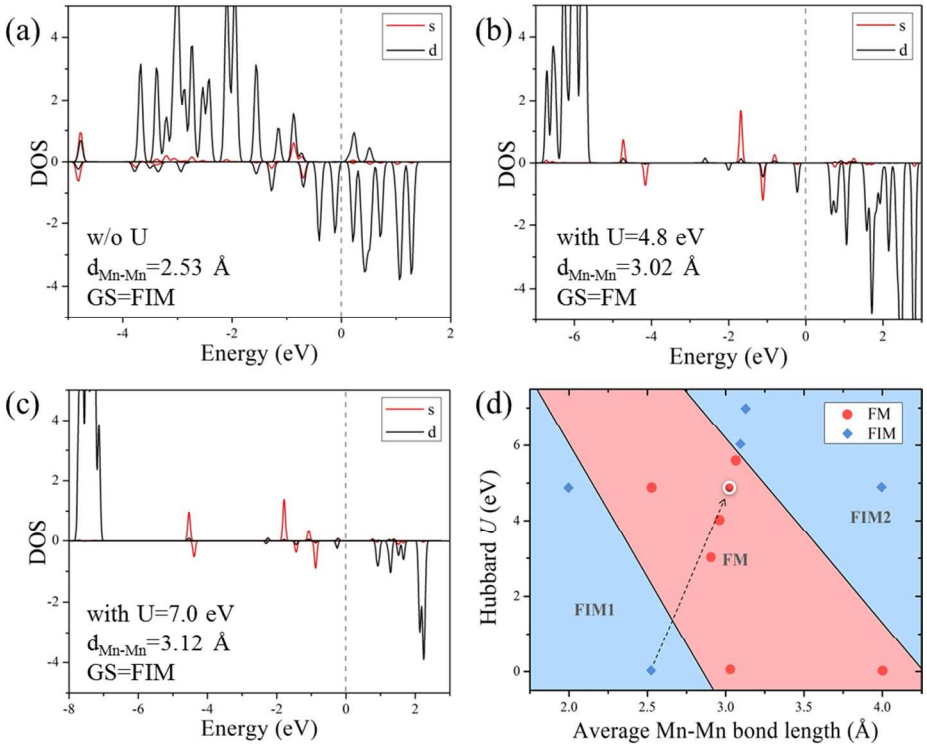

Figure 5. (a), (b), (c) Partial density of states of single Mn atom in Mn_5. (d) Magnetic phase diagram as a function of average Mn-Mn bond length and Hubbard *U* for Mn_5. Blue squares and red circles represent the calculated results with certain average Mn-Mn bond length and Hubbard *U*. The red circle with white frame represents the optimal result with Hubbard *U* of 4.8 eV. The black dashed arrow represents the trend of phase transition after including Hubbard *U*.

Now we consider charged Mn_2 and Mn_5 clusters to discuss the environmental influence on their magnetic states. For synthesizing cluster based materials, a cluster is usually adsorbed on a substrate[39] or ligated. Charge transfer between the cluster and the substrate or the ligands will leave the cluster charged either positively or negatively. Charged clusters are also produced in photoelectron spectroscopy experiment.[11] It is,

therefore, useful to know how the magnetic properties of a Mn cluster will change when supported or ligated. For Mn_2, when Hubbard U is not included, similar to neutral Mn_2, both Mn_2^- and Mn_2^+ show FM ground states, which are 0.33 and 0.28 eV lower than the AFM states. When Hubbard U of 4.8 eV is included, the AFM states of Mn_2^- and Mn_2^+ are 0.05 and 0.63 eV higher than the FM states. Our results agree with the experiment where Mn_2^+ is known to be ferromagnetic with a magnetic moment of 11 μ_B.

Figure 6 shows the geometries, spin moments and symmetry group of the optimal states for Mn_5^-, Mn_5 and Mn_5^+ calculated using DFT+U method. We find that the ground states of charged Mn_5 clusters also have different magnetic configurations. For Mn_5^-, the ground state is FIM (M2) with a total spin of 6 μ_B (1.2 μ_B/atom) and $d_{Mn\text{-}Mn}$ = 3.05 Å. The FM state lies 0.09 eV higher in energy. For Mn_5^+, the ground state is also FIM, where the three Mn atoms in the triangle have spins up and the two capped Mn atoms have spins down. The total spin moment becomes 4 μ_B (0.8 μ_B/atom) and the optimized $d_{Mn\text{-}Mn}$ is 3.03 Å. The FM coupling state is 0.1 eV higher in energy than the ground state. The relative energies of other possible magnetic configurations with the TBP geometry can be found in the supporting information. These results indicate that the magnetic state of Mn_5 cluster is sensitive to its chemical environment.

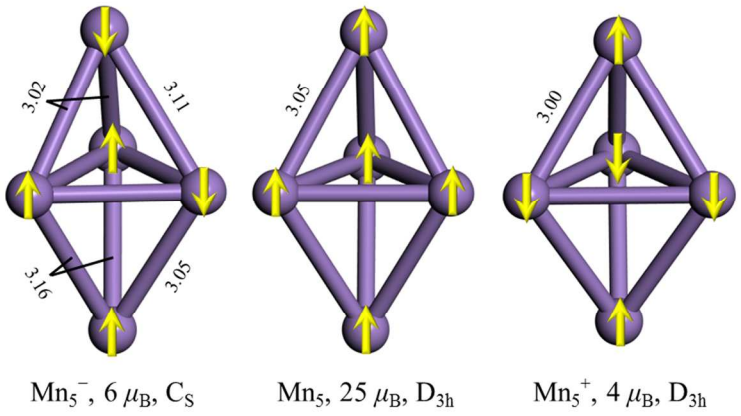

Figure 6. Optimized ground state of Mn_5^-, Mn_5, and Mn_5^+ calculated with Hubbard U of 4.8 eV. The bond lengths are represented in Å.

IV. Summary

In summary, our first-principles calculations reveal that in order to achieve the correct magnetic configuration of Mn clusters, strong correlation correction needs to be included. We incorporated this effect using the DFT+*U* method. Using the linear response theory, we calculated the Hubbard *U* to be 4.8 eV for the Mn_2 dimer and used the same value for clusters containing up to 5 atoms. We obtain an AFM ground state with a total spin moment of 0 μ_B and Mn-Mn distance of 3.34 Å for Mn_2, in good agreement with the experimental results. Using the same strategy, we demonstrate that the ground state of neutral Mn_5 is FM with a total spin moment of 25 μ_B and average Mn-Mn bond length of 3.02 Å. By analyzing their electronic structure, we show that addition of Hubbard *U* weakens the hybridization between *s* and *d* orbitals, which is responsible for the increase of Mn-Mn bond length, causing a transition in the magnetic states. A magnetic phase diagram is plotted to demonstrate the FIM1-to-FM-to-FIM2 transition along with Mn-Mn bond length and Hubbard *U*. We also show that the charged Mn_5 clusters (Mn_5^- and Mn_5^+) prefer FIM coupling rather than the FM coupling, in contrast to the results for Mn_2. In conclusion, it is important to include Hubbard *U* while calculating the magnetic properties of Mn nanostructures within the density functional theory.

Supporting Information Available: The linear response calculations for Hubbard *U*, the considered atomic and magnetic configurations and the corresponding energies of Mn_5, the HOMO and LUMO orbitals of Mn_2, magnetic states of Mn_5^- and Mn_5^+ and a Hubbard *U* test for Mn_2.

Acknowledgement

This work is partially supported by the U.S. Department of Energy, Office of Basic Energy Sciences, Division of Materials Sciences and Engineering under Award # DE-FG02-96ER45579. The work performed in NUST is supported by the NSFC (51522206, 11574151, 11774173), NSF of Jiangsu Province (BK20130031), PAPD, the Fundamental Research Funds for the Central Universities (No.30915011203), and New Century Excellent Talents in University (NCET-12-0628). C.H. acknowledges the China Scholarship Council (CSC) for sponsoring his visit to Virginia Commonwealth University (VCU) where this work was conducted. Resources of the National Energy Research Scientific Computing Center supported by the Office of Science of the U.S. Department of Energy under Contract no. DE-AC02-05CH11231 is also acknowledged.

References:

(1) Wolf, S. A.; Awschalom, D. D.; Buhrman, R. A.; Daughton, J. M.; Molnár, S.; von Roukes, M. L.; Chtchelkanova, A. Y.; Treger. D. M. Spintronics: A spin-based electronics vision for the future. Science 2001, 294, 1488-1495.

(2) Erwin, S. C.; Zu, L.; Haftel, M. I.; Efros, A. L.; Kennedy, T. A.; Norris, D. J. Doping semiconductor nanocrystals. Nature 2005, 436, 91-94.

(3) Baumann, C. A.; Van Zee, R. J.; Bhat, S. V.; Weltner Jr., W. ESR of Mn_2 and Mn_5 molecules in rare-gas matrices J. Chem. Phys. 1983, 78, 190-199.

(4) Nayak, S. K.; Jena, P. Anomalous magnetism in small Mn clusters. Chem. Phys. Lett. 1998, 289, 473-479.

(5) Nayak, S. K.; Rao, B. K.; Jena, P. Equilibrium geometries, electronic structure and magnetic properties of small manganese clusters. J. Phys.: Condens. Matter 1998, 10, 10863-10877.

(6) Pederson, M. R.; Reuse, F.; Khanna, S. N. Magnetic transition in Mn_n (n=2-8) clusters. Phys. Rev. B 1998, 58, 5632-5636.

(7) Desmarais, N.; Reuse, F. A.; Khanna, S. N. Magnetic coupling in neutral and charged Cr_2, Mn_2, and CrMn dimers. J. Chem. Phys. 2000, 112, 5576-5584.

(8) Bobadova-Parvanova, P.; Jackson, K. A.; Srinivas, S.; Horoi, M. Emergence of antiferromagnetic ordering in Mn clusters. Phys. Rev. A 2003, 67, 061202(R).

(9) Kabir, M.; Mookerjee, A. Structure, electronic properties, and magnetic transition in manganese clusters. Phys. Rev. B 2006, 73, 224439.

(10) Gutsev, G. L.; Mochena, M. D. Structure and Properties of Mn_n, Mn_n^-, and Mn_n^+ Clusters (n=3-10). J. Phys. Chem. A 2006, 110, 9758-9766.

(11) Gutsev, G. L.; Weatherford, C. A.; Ramachandran, B. R.; Gutsev, L. G.; Zheng, W.-J.; Thomas, O. C.; Bowen, Kit H. Photoelectron spectra and structure of the Mn_n^- anions (n = 2–16). J. Chem. Phys. 2015, 143, 044306.

(12) Barborini, M. Neutral, Anionic, and Cationic Manganese Dimers through Density Functional Theory. J. Phys. Chem. A 2016, 120, 1716-1726.

(13) Ludwig, G. W.; Woodbury, H. H.; Carlson, R. O. Spin resonance of deep level impurities in germanium and silicon. J. Phys. Chem. Solids 1959, 8, 490-492.

(14) Van Zee, R. J.; Baumann, C. A.; Bhat, S. V.; Weltner Jr, W. ESR of the high-spin (S = 25/2) Mn_5 molecule. J. Chem. Phys. 1982, 76, 5636-5637.

(15) Knickelbein, M. B. Magnetic ordering in manganese clusters. Phys. Rev. B 2004, 70, 014424.

(16) Yamada, T.; Kunitomi, N.; Nakai, Y.; Cox, D. E.; Shirane, G. Magnetic Structure of α-Mn. J. Phys. Soc. Jpn. 1970, 28, 615-627.

(17) Sliwko, V.; Mohn, P.; Schwarz, K. The electronic and magnetic structures of alpha- and beta-manganese. J. Phys.: Condens. Matter 1994, 6, 6557-6564.

(18) Buchachenko, A. A.; Chałasiński, G.; Szczęśniak, M. M. Electronic structure and spin coupling of the manganese dimer: The state of the art of ab initio approach. *J. Chem. Phys.* 2010, 132, 024312.

(19) Anisimov, V. I.; Aryasetiawan, F.; Lichtenstein, A. I. First-principles calculations of the electronic structure and spectra of strongly correlated systems: the LDA+ *U* method. J. Phys.: Condens. Matter 1997, 9, 767-808.

(20) Sato, K.; Bergqvist, L.; Kudrnovský, J.; Dederichs, P. H.; Eriksson, O.; Turek, I.; Sanyal, B.; Bouzerar, G.; Katayama-Yoshida, H.; Dinh, V. A. *et al.* First-principles theory of dilute magnetic semiconductors. Rev. Mod. Phys. 2010, 82, 1633.

(21) Kim, G.; Park, Y.; JoonHan, M.; Yu, J.; Heo, C.; Hee Lee, Y. Structure and magnetism of small Gd and Fe nanoclusters: LDA+*U* calculations. Solid State Commun. 2009, 149, 2058-2060.

(22) Filippone, F.; Mattioli, G.; Alippi, P.; Bonapasta, A. A. Clusters and Magnetic Anchoring Points in (Ga,Fe)N Condensed Magnetic Semiconductors. Phys. Rev. Lett. 2011, 107, 196401.

(23) Tao, K.; Zhou, J.; Sun, Q.; Wang, Q.; Stepanyuk, V. S.; Jena, P. Self-consistent determination of Hubbard *U* for explaining the anomalous magnetism of the Gd_{13} cluster. Phys. Rev. B 2014, 89, 085103.

(24) Zaanen, J.; Sawatzky, G. A. Systematics in band gaps and optical spectra of 3D transition metal compounds. J. Solid State Chem. 1990, 88, 8-27.

(25) Şaşioğlu, E.; Friedrich, C.; Blügel, S. Strength of the Effective Coulomb Interaction at Metal and Insulator Surfaces. Phys. Rev. Lett. 2012, 109, 146401.

(26) Cococcioni, M.; de Gironcoli, S. Linear response approach to the calculation of the effective interaction parameters in the LDA+U method. Phys. Rev. B 2005, 71, 035105.

(27) Perdew, J. P.; Burke, K.; Ernzerhof, M. Generalized Gradient Approximation Made Simple. Phys. Rev. Lett. 1996, 77, 3865.

(28) Perdew, J.; Wang. Y. J. Accurate and simple analytic representation of the electron-gas correlation energy. Phys. Rev. B 1992, 45, 13244.

(29) Giannozzi, P.; Baroni, S.; Bonini, N.; Calandra, M.; Car, R.; Cavazzoni, C.; Ceresoli, D.; Chiarotti, G. L.; Cococcioni, M.; Dabo, I. *et al.* QUANTUM ESPRESSO: a modular and open-source software project for quantum simulations of materials. J. Phys.: Condens. Matter 2009, 21, 395502.

(30) Kresse, G.; Hafner, J. Ab initio molecular dynamics for liquid metals. Phys. Rev. B 1993, 47, 558.

(31) Blöchl, P. E. Projector augmented-wave method. Phys. Rev. B 1994, 50, 17953.

(32) Dudarev, S. L.; Botton, G. A.; Savrasov, S. Y.; Humphreys, C. J.; Sutton, A. P. Electron-energy-loss spectra and the structural stability of nickel oxide: An LSDA+U study. Phys. Rev. B 1998, 57, 1505.

(33) Vosko, S. H.; Wilk, L.; Nusair, M. Accurate spin-dependent electron liquid correlation energies for local spin density calculations: a critical analysis. Can. J. Phys. 1980, 58, 1200-1211.

(34) Makov, G.; Payne, M. C. Periodic boundary conditions in ab initio calculations. Phys. Rev. B 1995, 51, 4014.

(35) Bier, K. D.; Haslett, T. L.; Krikwood, A. D.; Moskovits, M. The resonance Raman and visible absorbance spectra of matrix isolated Mn_2 and Mn_3. J. Chem. Phys. 1988, 89, 6-12.

(36) Grimme, S. Semiempirical gga-type density functional constructed with a long-range dispersion correction. J. Comp. Chem. 2006, 27, 1787-1799.

(37) Carole, D. Determination and prediction of the magnetic anisotropy of Mn ions. Chem. Soc. Rev., 2016, 45, 5834-5847.

(38) Das, G. P.; Rao, B. K.; Jena, P. Ferromagnetism in Mn-doped GaN: From clusters to crystals. Phys. Rev. B 2003, 68, 035207.

(39) Sachse, T.; Néel, N.; Meierott, S.; Berndt, R.; Hofer, W. A.; Kröger, J. Electronic and magnetic states of Mn_2 and Mn_2H on Ag(111). New J. Phys. 2014, 16, 063021.

TOC GRAPHIC